Quantum Effects in Higher-Order Correlators of a Quantum-Dot Spin Qubit

A. Bechtold, F. Li, K. Müller, T. Simmet, P.-L. Ardelt, J. J. Finley, and N. A. Sinitsyn

Phys. Rev. Lett. **117**, 027402 — Published 6 July 2016

DOI: 10.1103/PhysRevLett.117.027402

Quantum effects in higher order correlators of a quantum dot spin qubit

A. Bechtold,[1,*] F. Li,[2,3,*] K. Müller,[1,4] T. Simmet,[1] P.-L. Ardelt,[1] J. J. Finley,[1,†] and N. A. Sinitsyn[3,‡]

[1] *Walter Schottky Institut and Physik Department, Technische Universität München, 85748 Garching, Germany*
[2] *Center for Nonlinear Studies, Los Alamos National Laboratory, Los Alamos, New Mexico 87545 USA*
[3] *Theoretical Division, Los Alamos National Laboratory, Los Alamos, New Mexico 87545, USA*
[4] *E. L. Ginzton Laboratory, Stanford University, Stanford, California 94305, USA*

(Dated: June 16, 2016)

We measure time-correlators of a spin qubit in an optically active quantum dot beyond the second order. Such higher order correlators are shown to be directly sensitive to pure quantum effects that cannot be explained within the classical framework. They allow direct determination of ensemble and quantum dephasing times, T_2^* and T_2, using only repeated projective measurements and without the need for coherent spin control. Our method enables studies of purely quantum behavior in solid state systems, including tests of the Leggett-Garg type of inequalities that rule out local hidden variable interpretation of the quantum dot spin dynamics.

PACS numbers: 78.67.Hc, 71.70.Jp, 72.25.Rb, 03.67.Pp

Electronic spins in optically active quantum dots (QDs) have exhibited very long spin lifetimes T_1, extending beyond a millisecond [1, 2], and intrinsic dephasing times T_2 beyond one microsecond when subject to externally applied magnetic fields [3–5]. These properties, combined with the potential for ultrafast optical preparation and control [6–8], make QD spin qubits very attractive for quantum information processing [9]. However, long spin relaxation times do not necessarily predicate the ability of QD spins to process quantum information. Therefore, the ability of the spin to show quantum behavior during microsecond intervals is not a priori obvious.

According to the formalism of quantum mechanics, an unobserved system persists in arbitrary superpositions of classical states until the system is probed [10]. Therefore, the state of the system before performing a measurement is not classically defined, questioning the existence of a hidden variable theory rendering the outcome of the measurement deterministic. Bell showed [11] that it is possible to perform experiments to probe the realism of a quantum system free from the existence of such hidden variables. Leggett and Garg developed similar tests for correlators of variables at different points in time [12, 13]. A related effect is the dependence of the future system's evolution on the very fact that prior measurements have been performed irrespectively of the outcome of the measurement [14]. The observation of such *quantum measurement effects*, which would be impossible without a state vector collapse at the measurement process, can be used as a direct test of non-classical behavior. Such violation of the Leggett-Garg inequality was demonstrated in various physical systems such as superconducting qubits [15], photons [16], defect centers in diamond [17], nuclear magnetic resonance [18] and phosphorous impurities in silicon [19]. However, in experiments with QDs, this has hitherto been a complex task since it corresponds to measurements of unusual higher order correlators, which are very difficult to extract from the background noise.

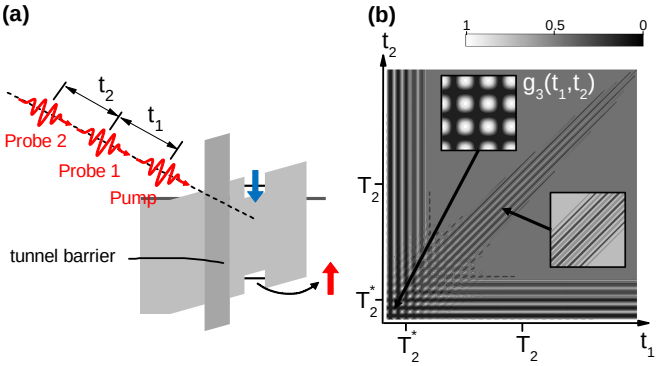

FIG. 1. (a) Band structure of voltage tunable spin memory device. The optical pump pulse prepares the electron in a spin down state, applications of optical probe pulses determine the electronic spin state at time moments t_1, $t_1 + t_2$. (b) Contour plot of $g_3(t_1, t_2)$ using Eq. (6). Insets show details of g_3 at timescales $t_{1,2} < T_2^*$ and $T_2^* < t_{1,2} < T_2$.

In this letter, we demonstrate entirely new methods to probe quantum measurement phenomena in semiconductor QD spin qubits. We introduce a measurement technique that can in principle determine an arbitrary order correlator $\langle \hat{Q}_{t_n+\ldots+t_1} \ldots \hat{Q}_{t_1} \hat{Q}_0 \rangle$, where the sub-indices indicate the time moments of application of the projection operator acting on the electronic spin, defined as $\hat{Q} \equiv |\downarrow\rangle \langle\downarrow|$. Here, $\langle \ldots \rangle$ indicates an averaging over many identical measurement sequences. In addition to direct evidence for the quantum nature of solid state qubits, we show that our method has practical importance since it provides a completely alternative route for measuring the coherence times of qubits which are typically measured through spin-echo techniques [20, 21] or methods in the frequency domain, such as coherent population trapping [22]. Such application of higher order correlators has been theoretically anticipated previously [23]

and can be applied to many other quantum systems in the solid state.

The basic idea of our experimental method is schematically illustrated in Fig. 1(a). An electron spin is first optically prepared in the $|\downarrow\rangle$-state in an individual InGaAs QD by using a picosecond laser pulse [3, 20], indicated by the label "Pump" in the figure, with a laser power corresponding to a Rabi-π-rotation that generates the neutral exciton state ($|cgs\rangle \rightarrow |\downarrow\Uparrow\rangle$). Immediately after exciton generation, the hole escapes the QD within 4 ps [20] leaving behind the single electron spin ($|\downarrow\Uparrow\rangle \rightarrow |\downarrow\rangle$). The implementation of an asymmetric tunnel barrier leads to electron lifetimes extending up to seconds whereas hole lifetimes are unaffected [1]. In our notation, such a spin selective electron preparation is equivalent to the nonzero outcome of the application of the projection operator $\hat{Q}_0$ at $t = 0$. Following the electron spin initiation, we apply one or more circularly polarized laser pulses, labeled "Probe 1" and "Probe 2" in Fig. 1(a), that probe the state of the spin at later moments ($t = t_1$ and $t = t_1 + t_2$), by taking advantage of optical spin selection rules in this system [7, 24]. Thus, if the electronic spin is in the state $|\uparrow\rangle$ at time t, such a probe pulse with a laser power corresponding to a Rabi-π-rotation excites an additional electron-hole pair ($|\uparrow\rangle \rightarrow |\uparrow\downarrow\Uparrow\rangle$), and the QD becomes charged with two electrons after hole tunneling ($|\uparrow\downarrow\Uparrow\rangle \rightarrow |2e\rangle$) and is, therefore, optically inactive during the remaining time. Such a state corresponds, in our notation, to the zero outcome of the measurements described by the projection operator $\hat{Q}_t$. On the other hand, if the electron spin is in the state $|\downarrow\rangle$ before the application of the probe pulse, the Pauli exclusion principle does not allow the excitation of a second electron-hole pair such that the QD becomes effectively transparent leaving behind a QD charged with one electron $|1e\rangle$.Finally, we perform the measurement of the total charge (1e or 2e) in the QD (not shown in Fig. 1(a)). Here, an observation of a doubly charged QD corresponds to at least one zero outcome of the measurements by operators $\hat{Q}_t$ (corresponding to at least one spin-flip event at t_1 or $t_1 + t_2$). Conversely, finding a singly charged QD at the end of the measurement sequence corresponds to the result $Q = 1$ in all measurement pulses (no spin-flip events at time instants t_1 and $t_1 + t_2$). All the relevant technical details pertaining to our sample and measurement method are presented in Ref. [25].

A simple model that illustrates quantum measurement effects is a spin in a fluctuating magnetic field applied along the x-axis, transverse to the measurement z-axis (Voigt configuration). This spin is described by the Hamiltonian:

$$\hat{H} = \omega(t)\hat{s}_x, \tag{1}$$

where $\omega(t)$ has a strong constant component due to the external field with Larmor frequency ω_L, and a fluctuating component due to the dynamics of the Overhauser field with frequency $\omega_O(t)$: $\omega(t) = \omega_L + \omega_O(t)$. The latter originates from hyperfine coupling to the bath of nuclear spins in the QD. It has nearly Gaussian statistics: $\langle\omega_O(t)\omega_O(t')\rangle = R(t-t')$, with correlation function $R(t)$. This model disregards feedback of the central spin dynamics on the nuclear spin bath, which was proven to be a good approximation due to strong nuclear quadrupole coupling [5, 20, 26]. We also disregard transverse Overhauser field components since their effect is suppressed due to fast spin precession in the yz-plane.

The Overhauser field has both fast and slow dynamics. Its fast fluctuations lead to irreversible loss of coherence with the effective spin lifetime T_2, while effects of the slow quasi-static part of $\omega_O(t)$ on spin correlators are analogous to the result of averaging over an ensemble of systems with different static fields and a characteristic ensemble dephasing time T_2^*.

Let $\hat{G}(t)$ be the evolution matrix for the measurement probabilities with an element $G_{\alpha\beta}(t)$, $\alpha, \beta \in \{\uparrow, \downarrow\}$, meaning the probability that after the system starts in the eigenstate with eigenvalue β of the spin projection operator on the z-axis, the measurement of the spin projection at a time t afterwards would find the spin in the state α, e.g.,

$$G_{\downarrow\downarrow}(t) = \frac{1}{2}\left(1 + \cos\left(\int_0^t \omega(t')\,dt'\right)\right). \tag{2}$$

The second and third order correlators of observable $\hat{Q} = |\downarrow\rangle\langle\downarrow|$ are then given by:

$$g_2(t) = \mathrm{Tr}\Big[\hat{Q}\hat{G}(t)\hat{Q}\Big], \tag{3}$$

$$g_3(t_1, t_2) = \mathrm{Tr}\Big[\hat{Q}\hat{G}(t_2)\hat{Q}\hat{G}(t_1)\hat{Q}\Big]. \tag{4}$$

Between measurements of the spin state, the presence of an external magnetic field leads to oscillations of the probability of observing $Q = 1$. Importantly, even if this value is observed, quantum measurement is generally destructive, i.e. it resets the density matrix to $|\downarrow\rangle\langle\downarrow|$. Measurements become nondestructive only when the time intervals t_1 and t_2 are chosen to be commensurate with the period of the spin precession. This situation corresponds to the quantum measurement effect of resonant enhancement of the correlator $g_3(t_1, t_2)$ [23]. We are going to show that it becomes especially pronounced in g_3 for times $t_2 = t_1 \gg T_2^*$.

Substituting Eq. (2) into Eqs. (3)-(4) and averaging the result over the Overhauser field distribution we find

$$g_2(t) = \frac{1}{2}\left(1 + \cos(\omega_L t)e^{-\frac{1}{2}\int_0^t dt_1 \int_0^t dt_2\, R(t_1 - t_2)}\right), \tag{5}$$

$$g_3(t_1, t_2) = \frac{1}{2}\left[g_2(t_1) + g_2(t_2) + \frac{1}{2}g_2(t_1 + t_2)\right] - \frac{3}{8} +$$

$$+\frac{1}{8}\cos(\omega_L(t_1-t_2))e^{-\int_0^{t_1+t_2}dt'\int_0^{t_1+t_2}dt''\frac{q(t')q(t'')}{2}R(t'-t'')} \quad (6)$$

Here, $q(t)=1$ for $t<t_1$ and $q(t)=-1$ for $t>t_1$. Figure 1(b) shows an example of $g_3(t_1,t_2)$ calculated using Eq. (6), considering the case of a correlator $R(t-t')=(1/T_2^*)^2+(2/T_2)\delta(t-t')$ [23, 25]. The corresponding correlators $g_2(t)$ in Eq. (5), and hence the term $[\ldots]$ in Eq. (6), decay quickly during T_2^* [25]. The insets in Fig. 1(b) show details of g_3 at small ($t_{1,2}<T_2^*$) and large ($t_{1,2}>T_2^*$) timescales. Remarkably, the last term in Eq. (6) along the diagonal direction for $t_1=t_2$ survives for timescales much longer than T_2^*. Without a collapse of the wave function by the measurement, g_3 would also decay quickly for $T_2^*<t_{1,2}\ll T_2$ to a constant value 1/4 [25]. However, the 3$^{\rm rd}$ order correlator is influenced by quantum measurement effects [25] that make the last term in Eq. (6) immune to inhomogeneous broadening for equal time intervals between successive measurements. Along the line $t_1=t_2\equiv t$, the correlator g_3 first decays quickly within the time T_2^*, then it decays slowly at timescales of T_2 according to $\sim e^{-2t/T_2}$ towards the value of 1/4 [25]. In fact, one can recognize the exponent in the last term in Eq. (6), at $t_1=t_2$, as the expression that describes the spin echo amplitude in our model [27].

Experiment. Typical measurements of g_2 and g_3 are presented in Fig. 2(a) and (b), respectively, for timescales where $t_{1,2}$ are in the nanosecond range. Figure 2(a) shows that the amplitude of $g_2(t)$ oscillates with the Larmor

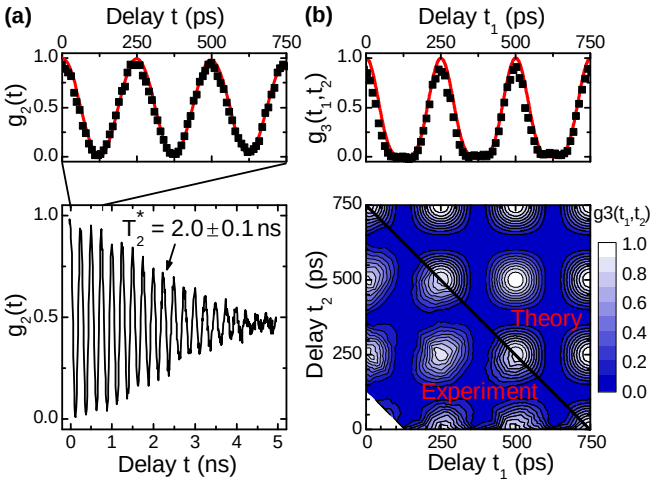

FIG. 2. (a) Experimental data of $g_2(t)$ at in-plane magnetic fields of $B_x=0.5$ T with zoom-in over the initial time. Inhomogeneous dephasing takes place after 2 ns owing to contributions of randomly orientated Overhauser fields. (b) Experimental data of $g_3(t_1,t_2)$. The upper part shows a line cut of the contour plot along the anti-diagonal direction, keeping the total time fixed to $t_1+t_2=750$ ps. Comparison with theoretical predictions using Eq. (6) (red line and upper part of contour plot).

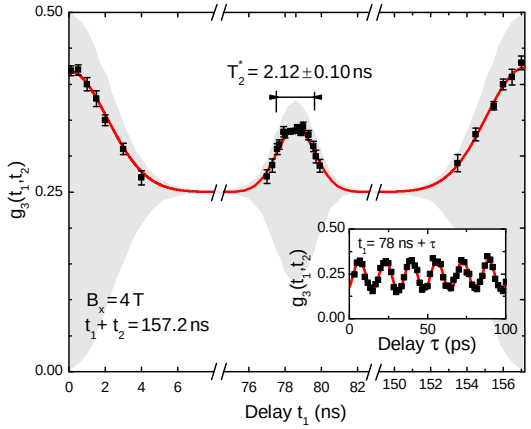

FIG. 3. Experimental data for g_3 along the direction $t_1+t_2=157.2$ ns (anti-diagonal) at $B_x=4$ T. The shaded area indicates the envelope of g_3 oscillations with probe fidelities equal to unity. The data points are obtained by analyzing the oscillation amplitude, as shown in the inset, using a sinusoidal fit (red line) at different time sections of t_1-traces.

frequency ($|g_e|=0.55$), since an in-plane magnetic field of $B_x=0.5$ T is applied. Within the initial 2.0 ns the amplitude of g_2 quickly decays with a Gaussian envelope as $\sim e^{-\frac{1}{2}(t/T_2^*)^2}$ owing to contributions of randomly oriented Overhauser fields [20, 28–30]. The red line shows the application of Eq. (5) agreeing very well with the experimental results. This demonstrates the high fidelity of our spin initialization and readout methods, a necessary pre-requisite for conducting higher order correlation measurements. In contrast to the sinusoidal behavior of g_2, the correlator g_3 obtained using a three pulse experiment shows a pattern that is comparable to $g_2(t_1)g_2(t_2)$ at such short timescales. A typical result is presented in Fig. 2(b) that agrees very well with the theoretical predictions of Eq. (6) (red line and contour plot).

At longer timescales $T_2^*<t_{1,2}<T_2$, i.e. at hundreds of nanoseconds, the decay of the oscillation amplitude of g_3 along the anti-diagonal direction reflects the dephasing time T_2^*, according to Eq. 6. In order to demonstrate this experimentally, we keep the total time $t_1+t_2=157.2$ ns fixed and tune only the time delay t_1. The result of analyzing the oscillation amplitude of g_3 along such an anti-diagonal line is shown in Fig. 3 at $B_x=4$ T. The inset in Fig. 3 resolves details of g_3 from which the oscillation amplitude is obtained. Notably, the oscillation amplitudes at time instants $t_1\simeq t_2$ have non-vanishing components for $t_{1,2}\gg T_2^*$ and, hence, are different from classical values according to $g_2(t_1)g_2(t_2)=1/4$, which reflects the quantum nature of the correlator g_3 [25]. From the width of the Gaussian-like envelope we extract $T_2^*=2.12\pm0.10$ ns, in agreement with values obtained by measuring the g_2 spin correlator, shown in Fig. 2(a).

The amplitude of g_3 along the diagonal direction ($t_1=t_2=t$) as a function of the total time $2t$ is presented in

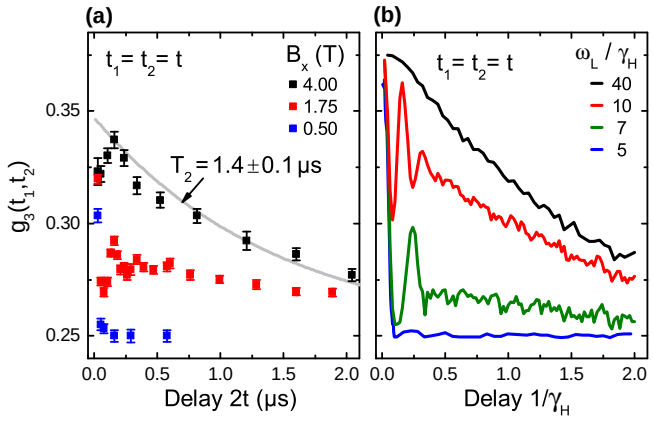

FIG. 4. (a) Experimental data of $g_3(t,t)$ along $t_1 = t_2$ direction for different magnetic fields B_x. (b) Numerically obtained $g_3(t,t)$ at different magnetic fields. The numerical time is in units of inverse average hyperfine coupling $1/\gamma_H$ of a single nuclear spin [25], and magnetics field are in units of ω_L/γ_H. The number of simulated nuclear spins is $N = 900$.

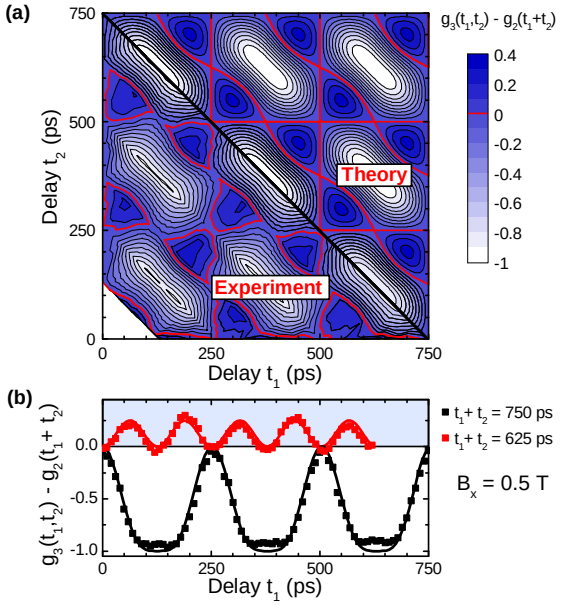

FIG. 5. (a) Contour plot of $g_3(t_1,t_2) - g_2(t_1+t_2)$ at $B_x = 0.5$ T. The area within the red contour correspond to data points which violate Eq. (7) and is in very good agreement with theoretical modeling. (b) Experimental data (dots) and theoretical calculation (solid line) corresponding to line-cuts in (a) for $t_1 + t_2 = 690$ ps and 750 ps, respectively.

Fig. 4(a) for different magnetic fields. At high magnetic fields ($B_x = 4$ T) the correlator $g_3(t,t)$ decays monoexponentially with $T_2 = 1.4 \pm 0.1$ μs (gray line), i.e., much slower than T_2^*. It can be seen that upon reducing the magnetic field to $B_x = 1.75$ T, $g_3(t,t)$ exhibits slowly oscillatory behavior in addition to an overall decay, whereas at $B_x = 0.5$ T a relatively fast decay takes place towards the limit of 1/4 after ~ 40 ns. The slowly oscillatory behavior is contrary to predictions of the model with only two lifetimes, but comparable to features observed in spin echo measurements [5, 20, 31].

To account for this behavior, a more rigorous model of decoherence by a nuclear spin bath must include effects of hyperfine and quadrupole interactions on central spin dynamics, including both quadrupole and hyperfine couplings and the feedback from central spin dynamics on nuclear spins. For this, we simulated coupling to nuclear spins numerically within the dynamical mean field algorithm [32], as described in detail in Refs. [20, 25]. The results of numerical calculations, presented in Fig. 4(b), show qualitatively similar behavior to the experimentally observed data for $g_3(t,t)$. This confirms that the oscillations of $g_3(t,t)$ at magnetic fields below 4 T can be explained by the presence of quadrupole interactions in the nuclear spin bath, in agreement with Refs. [5, 20, 31].

Leggett-Garg type inequality. Pure quantum behavior of the correlator $g_3(t_1,t_2)$ can be also revealed if we note that, in classical physics, an application of any extra probe pulse would only reduce the probability for a QD to remain in the 1e-charge state at the end of the measurement sequence. Indeed, imagine that the spin is always physically present in one of the states $|\uparrow\rangle$ or $|\downarrow\rangle$, and there is a hidden variable theory that leads to the existence of a joint probability $p_{\alpha,\beta}(t_2+t_1,t_1)$ of observing the values $\alpha,\beta \in \{0,1\}$ at time moments $t_1 + t_2$ and t_1. Then $\langle \hat{Q}_{t_2+t_1} \hat{Q}_{t_1} \rangle \leq \langle \hat{Q}_{t_1+t_2} \rangle$ and we arrive at a constraint on the correlators of $Q \in \{0,1\}$:

$$g_3(t_2,t_1) \leq g_2(t_1+t_2). \qquad (7)$$

This relation is of the same origin as the Leggett-Garg inequalities, which are usually formulated for dichotomous variables taking values in $\{-1,1\}$ [12]. The result of using Eq. (7) on our measurement data is presented in Fig. 5(a) for $B_x = 0.5$ T, where positive values correspond to a violation of the inequality (7) (region within the red line in the contour plot). In Fig. 5(b), two cross sections through the experimental data from (a) are presented for $t_1 + t_2 = 690$ ps and 750 ps (data points), together with the corresponding theoretical calculations that assume coherent spin precession (solid lines). The values corresponding to $g_3(t_1,t_2) - g_2(t_1+t_2) > 0$ are classically forbidden and demonstrate that the dynamics of a single electron spin cannot be described by a classical theory with hidden variables.

In conclusion, we demonstrated that fully optical preparation and readout schemes of the electron spin states in an optically active QD make it possible to measure spin qubit time-correlators beyond the second order (g_2). Our results revealed effects that were entirely incompatible with a classical nondestructive measurement framework. They can be used as an alternative to spin echo or dynamic decoupling approaches to determine the ensemble and intrinsic dephasing times, T_2^* and T_2, without using coherent spin control sequences. We also ob-

served deviations of such correlators from predictions of phenomenological models based on several characteristic lifetimes, which revealed even more subtle details of qubit interaction with the environment.

We gratefully acknowledge financial support from the DFG via SFB-631, Nanosystems Initiative Munich, the EU via S3 Nano and BaCaTeC. K.M. acknowledges financial support from the Alexander von Humboldt foundation and the ARO (grant W911NF-13-1-0309). Work at LANL was supported by the U.S. Department of Energy, Contract No. DE-AC52-06NA25396, and the LDRD program at LANL.

* these authors contributed equally to this work
† email: jonathan.finley@wsi.tum.de
‡ email: nsinitsyn@lanl.gov

[1] D. Heiss, V. Jovanov, M. Caesar, M. Bichler, G. Abstreiter, and J. J. Finley, Appl. Phys. Lett. **94,** 072108 (2009).
[2] A. V. Khaetskii, D. Loss, and L. Glazman, Phys. Rev. Lett. **88,** 186802 (2002).
[3] D. Press, K. De Greve, P. L. McMahon, T. D. Ladd, B. Friess, C. Schneider, M. Kamp, S. Höfling, A. Forchel, and Y. Yamamoto, Nature Photon. **4,** 367 (2010).
[4] H. Bluhm, S. Foletti, I. Neder, M. Rudner, D. Mahalu, V. Umansky, and A. Yacoby, Nature Phys. **7**, 109 (2010).
[5] R. Stockill, C. Le Gall, C. Matthiesen, L. Huthmacher, E. Clarke, Maxime Hugues, and M. Atature, arXiv preprint arXiv:1512.01811 (2015).
[6] A. Greilich, S. G. Carter, D. Kim, A. S. Bracker, and D. Gammon, Nature Photon. **5**, 702 (2011).
[7] S. E. Economou, and T. L. Reinecke, Phys. Rev. Lett. **99,** 217401 (2007).
[8] T. M. Godden, J. H. Quilter, A. J. Ramsay, Yanwen Wu, P. Brereton, S. J. Boyle, I. J. Luxmoore, J. Puebla-Nunez, A. M. Fox, and M. S. Skolnick, Phys. Rev. Lett. **108**, 017402 (2012).
[9] T. D. Ladd, F. Jelezko, R. Laflamme, Y. Nakamura, C. Monroe, and J. L. OBrien, Nature **464,** 45 (2010).
[10] E. Schrödinger, Naturwissenschaften **23,** 807 (1935).
[11] J. S. Bell, Physics 1, **3,** 195 (1964).
[12] A. J. Leggett, and A. Garg, Phys. Rev. Lett. **54**, 857 (1985).
[13] C. Emary, N. Lambert, and F. Nori, Rep. Prog. Phys. **77,** (2014).
[14] L. Clemente, and J. Kofler, Phys. Rev. A **91**, 062103 (2015).
[15] A. Palacios-Laloy, F. Mallet, F. Nguyen, P. Bertet, D. Vion, D. Esteve, and A. N. Korotkov, Nat. Phys. **6**, 442 (2010).
[16] M. E. Goggin, M. P. Almeida, M. Barbieri, B. P. Lanyon, J. L. OBrien, A. G. White, and G. J. Pryde, Proc. Natl. Acad. Sci. USA **108**, 1256 (2011).
[17] R. E. George, L. M. Robledo, O. J. E. Maroney, M. S. Blok, H. Bernien, M. L. Markham, D. J. Twitchen, J. J. L. Morton, G. A. D. Briggs, and R. Hanson, Proc. Natl. Acad. Sci. USA **110**, 3777 (2013).
[18] V. Athalye, S. S. Roy, and T. S. Mahesh, Phys. Rev. Lett. **107**, 130402 (2011).
[19] G. C. Knee, S. Simmons, E. M. Gauger, J. J. Morton, H. Riemann, N. V. Abrosimov, P. Becker, H.-J. Pohl, K. M. Itoh, M. L. Thewalt, G. A. D. Briggs, and S. C. Benjamin, Nat. Commun. **3**, 606 (2012).
[20] A. Bechtold, D. Rauch, F. Li, T. Simmet, P.-L. Ardelt, A. Regler, K. Müller, N. A. Sinitsyn, and J. J. Finley, Nature Phys. **11,** 1005 (2015).
[21] K. De Greve, P. L. McMahon, D. Press, T. D. Ladd, D. Bisping, C. Schneider, M. Kamp, L. Worschech, S. Höfling, A. Forchel, and Y. Yamamoto, Nature Phys. **7,** 872 (2011).
[22] X. Xu, B. Sun, P. R. Berman, D. G. Steel, A. S. Bracker, D. Gammon, and L. J. Sham, Nat. Phys. **4**, 692 (2008)
[23] R.-B. Liu, S.-H. Fung, H.-K. Fung, A. N. Korotkov, and L. J. Sham, New J. Phys. **12**, 013018 (2010).
[24] M. Bayer, G. Ortner, O. Stern, A. Kuther, A. A. Gorbunov, A. Forchel, P. Hawrylak, S. Fafard, K. Hinzer, T. L. Reinecke, S. N. Walck, J. P. Reithmaier, F. Klopf, and F. Schäfer, Phys. Rev. B **65**, 195315 (2002).
[25] See Supplemental Material, which includes Refs. [33-35].
[26] N. A. Sinitsyn, Y. Li, S. A. Crooker, A. Saxena, and D. L. Smith, Phys. Rev. Lett. **109**, 166605 (2012).
[27] See, e.g., Supplemental Material in [20]. We believe, however, that this coincidence is the result of the model simplicity. Generally, correlator representing spin echo effect is different from $g_3(t,t)$.
[28] I. A. Merkulov, A. L. Efros, and M. Rosen, Phys. Rev. B **65**, 205309 (2002).
[29] W. Zhang, V. V. Dobrovitski, K. A. Al-Hassanieh, E. Dagotto, and B. N. Harmon, Phys. Rev. B **74**, 205313 (2006).
[30] C. Testelin, F. Bernardot, B. Eble, and M. Chamarro, Phys. Rev. B **79**, 195440 (2009).
[31] J. Hackmann, P. Glasenapp, A. Greilich, M. Bayer, and F. B. Anders, Phys. Rev. Lett. **115,** 207401 (2015).
[32] K. A. Al-Hassanieh, V. V. Dobrovitski, E. Dagotto, and B. N. Harmon, Phys. Rev. Lett. **97**, 037204 (2006).
[33] F. H. L. Koppens, J. A. Folk, J. M. Elzerman, R. Hanson, L. H. Willems van Beveren, I. T. Vink, H. P. Tranitz, W. Wegscheider, L. P. Kouwenhoven, and L. M. K. Vandersypen, Science **309**, 1346–1350 (2005)
[34] A. Zrenner, E. Beham, S. Stufler, F. Findeis, M. Bichler, and G. Abstreiter, Nature **418**, 612–614 (2004).
[35] P. L. Ardelt, T. Simmet, K. Mueller, C. Dory, K. A. Fischer, A. Bechtold, A. Kleinkauf, H. Riedl, and J. Finley, Phys. Rev. B **92**, 115306 (2015).